

Electronic Supplementary Information

Constructing one-dimensional silver nanowire-doped reduced graphene oxide integrated with CdS nanowire network hybrid structures toward artificial photosynthesis

Siqi Liu,^{a,b} Bo Weng,^{a,b} Zi-Rong Tang,^{b*} and Yi-Jun Xu^{a,b*}

^a State Key Laboratory of Photocatalysis on Energy and Environment, College of Chemistry, Fuzhou University, Fuzhou, 350002, P. R. China

^b College of Chemistry, Fuzhou University, New Campus, Fuzhou, 350002, P. R. China

*To whom correspondence should be addressed E-mail: zrtang@fzu.edu.cn ; yjxu@fzu.edu.cn

Experimental Section

1 Preparation.

Materials. Sodium diethyldithiocarbamate trihydrate ($C_5H_{10}NNaS_2 \cdot 3H_2O$), cadmium chloride ($CdCl_2 \cdot 2.5H_2O$), ethylenediamine ($C_2H_8N_2$), sulfuric acid (H_2SO_4), hydrochloric acid (HCl), hydrogen peroxide, 30% (H_2O_2), potassium permanganate ($KMnO_4$), silver nitrate ($AgNO_3$), ferric chloride ($FeCl_3$), (3-aminopropyl)triethoxysilane (APTES), polyvinylpyrrolidone (PVP, $M_w = 300000$), ethanol (C_2H_6O), and ethylene glycol ($C_2H_6O_2$) were obtained from Sinopharm Chemical Reagent Co., Ltd. (Shanghai, China). Flake graphite powder were obtained from Qingdao Zhongtian Company, China. All materials were analytical grade and used as received without further purification. Deionized water used in the synthesis was from local sources.

Synthesis. The reduced graphene oxide–CdS nanowires (CG) and reduced graphene oxide–Ag nanowires–CdS nanowires nanocomposites (ACG) were fabricated by a simple and efficient electrostatic self-assembly method followed by a hydrothermal reduction process.^{S1} *(I) Fabrication of CdS nanowires (CdS NWs).* Uniform CdS NWs were grown through a modified method.^{S2-4} In a typical process, 1.124 g of cadmium diethyldithiocarbamate ($Cd(S_2CNEt_2)_2$), prepared by precipitation from a stoichiometric mixture of sodium diethyldithiocarbamate trihydrate and cadmium chloride in deionized water, was added to a Teflon-lined stainless steel autoclave with a capacity of 50 ml. Then, the autoclave was filled with 40 ml of ethylenediamine to about 80% of the total volume. The autoclave was maintained at 180 °C for 24 h and then allowed to cool to room temperature. A yellowish precipitate was collected and washed with absolute ethanol and deionized water to remove residue of organic solvents. The final products were dried in oven at 60 °C for 12 h. *(II) Synthesis of Graphene Oxide (GO).* GO was synthesized from powdered flake graphite (400 mesh) by a modified Hummers method that involves a strong oxidation process in solution.^{S5} In detail, 10 g of graphite powder (supplied from Qingdao Zhongtian Company, China) was put into 230 mL of concentrated H_2SO_4 under moderate stirring, and the solution was cold below 5 °C in an ice bath. 30 g of $KMnO_4$ was added gradually under stirring and the temperature of the mixture was kept to be below 20 °C by cooling. Then, the solution was heated to 35 °C in a water-bath kept stirring for 2 h. Successively, the mixture was diluted with

500 ml of DI water in an ice bath to keep the temperature below 50 °C for 10 min. Shortly after the further diluted with 1.5 L of DI water, 80 ml of 30% H₂O₂ was then added to the mixture and a yellow brown product was formed along with bubbling. The mixture was centrifuged and washed with 1:10 HCl aqueous solution to remove metal ions followed by DI water (six times) to remove the acid. After that, the mixture was dialyzed for a week and followed by a dry at 60 °C to get the final graphene oxide sample. (III) *Fabrication of Ag nanowires (Ag NWs)*. For a typical synthesis of Ag NWs, an one-pot reaction was employed to mix all compounds and solvents.^{S6} Briefly, 0.2 g of PVP (M_w = 300000) was first added to 25 ml of ethylene glycol (EG) and completely dissolved using magnetic stirring at room temperature. Afterwards, 0.25 g of silver nitrate (AgNO₃) was added to the PVP solution. Complete dissolution was required to obtain a transparent and uniform solution. Finally, 3.5 g of a FeCl₃ salt solution (600 μM in EG) was dumped into the mixture and stirred for one or two minutes. The mixture was then immediately transferred into a preheating to 130 °C reactor to grow Ag NWs for 5 h until the reaction was complete. Afterwards, acetone and ethanol were used to wash the precipitate with centrifugation of 4000 rpm for 5 min. Finally, the Ag NWs were redispersed in ethanol for future use. (IV) *Synthesis of Ag NWs–GO by electrostatic self-assembly of Ag NWs on the GO*. A 0.4 g portion of Ag NWs was first dispersed in 200 ml of ethanol by sonication for 30 min. APTES (2 ml) was then added, heated, and refluxed at 60 °C for 4 h.^{S3} APTES-treated Ag NWs were sufficiently rinsed with ethanol to wash away any remaining APTES moiety. Then, the positively charged Ag NWs was added into the negatively charged GO suspension in water (0.2 mg·ml⁻¹) under vigorous stirring. After mixing for 2 min, the mixture was centrifuged and redispersed in deionized water. (V) *Synthesis of CG and ACG via electrostatic self-assembly method*. The given amounts of CdS NWs were dispersed in deionized water by sonication for 10 min. Then, negatively charged GO or Ag NWs–GO suspensions in water were added into the positively charged CdS NWs dispersion drop by drop with different weight addition ratios of GO or Ag NWs–GO (0.5, 1, 2, 5, 10 wt%) under vigorous stirring. After mixing for 30 min, the mixture was centrifuged and washed with deionized water. For the reduction of GO to RGO, a hydrothermal process was used as follows. The given amounts of CdS NWs–GO nanocomposites or CdS NWs–Ag NWs–GO nanocomposites were dispersed in deionized water, then autoclaved in a Teflon-lined stainless steel vessel at 110 °C for 14 h. The dark green precipitates were collected, washed with deionized water, and then dried in oven at 60 °C.

2 Characterization.

Zeta potentials (ξ) measurements of the samples were determined by dynamic light scattering analysis (Malvern Zetasizer Nano—ZS90) at room temperature of 25 °C. The crystal phase properties of the samples were analyzed with a Bruker D8 Advance X-ray diffractometer (XRD) using Ni-filtered Cu Kα radiation at 40 kV and 40 mA in the 2θ ranging from 10° to 80° with a scan rate of 0.02° per second. The optical properties of the samples were analyzed using a UV–vis spectrophotometer (Cary-500, Varian Co.) in which BaSO₄ was used as the background. Scanning electron microscopy (SEM) images were presented using an SU8000 instrument (Hitachi) with an accelerated voltage of 7 kV. The Fourier transformed infrared spectroscopy (FT-IR) was performed on a Nicolet Nexus 670 FT-IR spectrophotometer at a resolution of 4 cm⁻¹. Raman spectroscopic measurements were performed on a Renishaw inVia Raman System 1000 with a 532 nm Nd:YAG excitation source at room temperature. The Brunauer–Emmett–Teller (BET) specific surface area (S_{BET}) of the samples was analyzed by nitrogen (N₂) adsorption–desorption in a Micromeritics ASAP 2020 apparatus. The photoluminescence (PL) spectra for solid samples were investigated on an Edinburgh FL/FS920 spectrophotometer with an excitation wavelength of 380 nm. For PL decay measurements, the light-emitting diode lamp was used to get the laser beam with excitation wavelengths of 405 nm. The 405 nm laser beam at an incident angle of ~45° relative to the normal direction was focused onto the samples at room

temperature. The fluorescence signal was collected vertically from the sample surface sent through a FLS980 Fluorescence Spectrometer for spatial and spectral PL characterizations or to an avalanche photo diode for the PL decay measurements using a time-correlated single-photon counting system. Emission lifetimes were analyzed by the use of a program for exponential fits. The photocurrent measurements were performed in homemade three electrode quartz cells with a PAR VMP3 Multi Potentiostat apparatus. The electrolyte was 0.2 M aqueous Na_2SO_4 solution (pH = 6.8) without additive. The electrochemical impedance spectroscopy (EIS) and measurements were performed in the presence of 10 mM $\text{K}_3[\text{Fe}(\text{CN})_6]/\text{K}_4[\text{Fe}(\text{CN})_6]$ and 0.5 M KCl by applying an AC voltage with 5 mV amplitude in a frequency range from 1 Hz to 100 kHz under open circuit potential conditions. The cyclic voltammograms were measured in 10 mM $\text{K}_3[\text{Fe}(\text{CN})_6]/\text{K}_4[\text{Fe}(\text{CN})_6]$ and 0.5 M KCl as a redox probe with the scanning rate of 20 mV/s in the same three-electrode cell as EIS measurement.

3 Photocatalytic activity

3.1 Selective reduction of nitroaromatic compounds.

The photocatalytic selective reduction of nitro-aromatic compounds to amino-aromatic compounds was performed in a self-designed photochemical reactor equipped with an electromagnetic stirrer. In a 100 ml glass flask equipped with a magnetic stir bar and a three-hole plug, 7 mg of catalyst was dispersed in 30 ml of a 20 $\text{mg}\cdot\text{L}^{-1}$ aqueous solution of nitroaromatic compounds with 30 mg of ammonium formate as hole scavenger. The mixture was stirred in the dark for 1 h to ensure the establishment of adsorption-desorption equilibrium between the sample and reactant. Then, the above suspension was irradiated with a 300 W Xe arc lamp (PLS-SXE 300, Beijing Perfect Light Co., Ltd.) with a UV-cut filter to cut off light with a wavelength $\lambda < 420$ nm. During the process of the reaction, 4 mL of sample solution was taken from the reaction system at a certain time interval. Then, the solid photocatalyst was immediately separated from the mixed phase by centrifugation, and the remaining supernatant was analyzed on a Varian UV-vis spectrophotometer (Cary 50, Varian Co.). The whole experimental process was conducted under N_2 bubbling at the flow rate of 80 $\text{mL}\cdot\text{min}^{-1}$. The photograph of the experimental setup was displayed in the follows (**Fig. S1†**).

3.2 Photocatalytic water splitting to H_2 .

Photocatalytic water splitting to H_2 was carried out in a Pyrex top-irradiation reaction vessel connected to a glass closed gas circulation system. H_2 evolution analysis was performed by dispersing 40 mg of catalyst powder in an aqueous solution (100 ml) containing lactic acid (10 ml) as the sacrificial electron donor. The reactant solution was evacuated several times to remove air completely before the photocatalytic reaction. A 300 W Xe arc lamp (PLS-SXE 300, Beijing Perfect Light Co., Ltd.) was applied as the light source, and visible light irradiation was realized by using a 420 nm cutoff filter. The temperature of the reactant solution was maintained at room temperature by a flow of cooling water during the reaction. The evolved gases were analyzed by gas chromatography. The photograph of the experimental setup was displayed in the follows (**Fig. S2†**).

3.3 Photocatalytic reduction of CO_2 .

Photocatalytic reduction of CO_2 in the presence of H_2O was carried out in a stainless-steel reactor (volume, ~100 ml) with a quartz window on the top of the reactor. The light source was 300 W Xe arc lamp (PLS-SXE 300, Beijing Perfect Light Co., Ltd.) with a UV-cut filter to cut off light with a wavelength $\lambda < 420$ nm. The photocatalytic reaction was performed in a gas (vapor)-solid heterogeneous reaction mode. Typically, 20 mg of solid catalyst was placed on a Teflon catalyst holder in the upper region of the reactor. Liquid water with a volume of 4 ml was pre-charged in the bottom of the reactor. It should be noted that the catalyst was not

immersed into the liquid water. Instead, the catalyst was surrounded by H_2O vapor and CO_2 . The pressure of CO_2 was typically regulated to 0.2 MPa. The temperature of the reactor was kept at 323 K, and the vapor pressure of H_2O was 12.3 kPa under such a circumstance. The photocatalytic reaction was typically performed for 2 h. The amounts of CO and CH_4 formed were analyzed by gas chromatography. We adopted a flame ionization detector (FID) for quantifying the amounts of CO and CH_4 formed from CO_2 to ensure high sensitivities. After the effluents containing CO_2 , CO and CH_4 were separated by a carbon molecular sieve (TDX-01) column, CO and CO_2 were further converted to CH_4 by a methanation reactor, and were then analyzed by the FID detector. The detection limits of our analytic method for CH_4 and CO were both 2 nmol (0.002 μmol). The photograph of the experimental setup was displayed in the follows (**Fig. S3†**).



Fig. S1 Photograph of the experimental setup for photocatalytic reduction of nitroaromatic compounds.



Fig. S2 Photograph of the experimental setup for photocatalytic water-splitting to hydrogen.



Fig. S3 Photograph of the experimental setup for photocatalytic gas-phase carbon dioxide reduction.

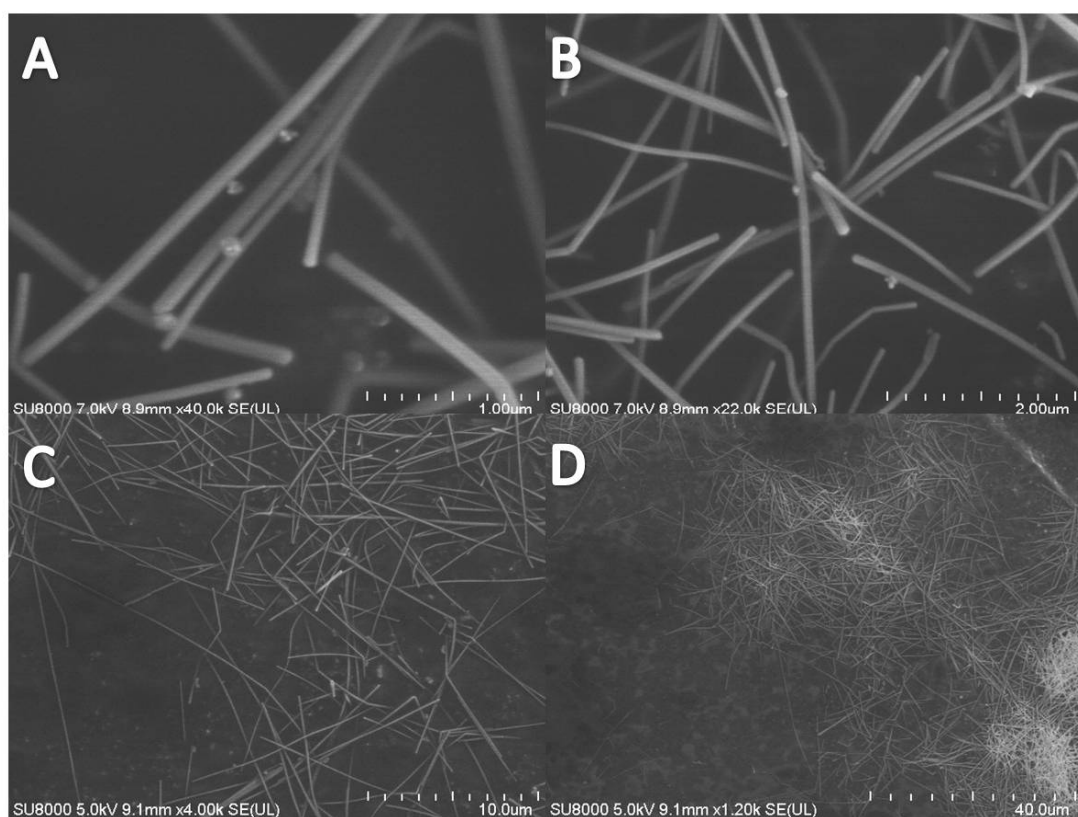


Fig. S4 Typical SEM images of Ag nanowires at different magnifications.

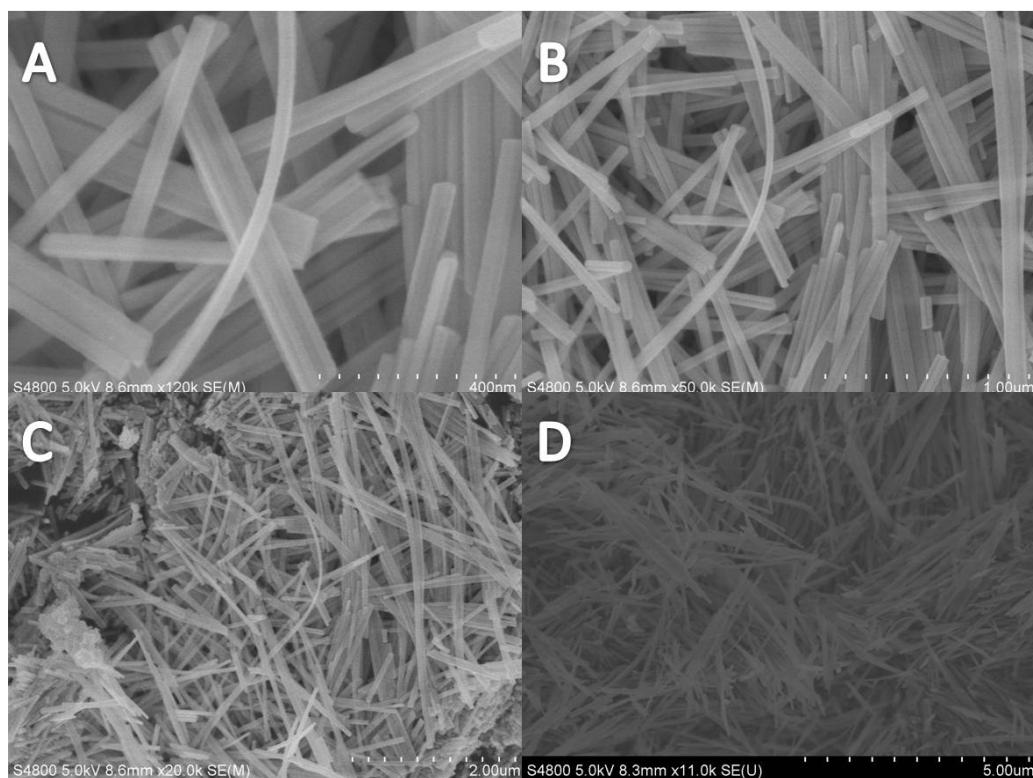


Fig. S5 Typical SEM images of CdS nanowires at different magnifications.

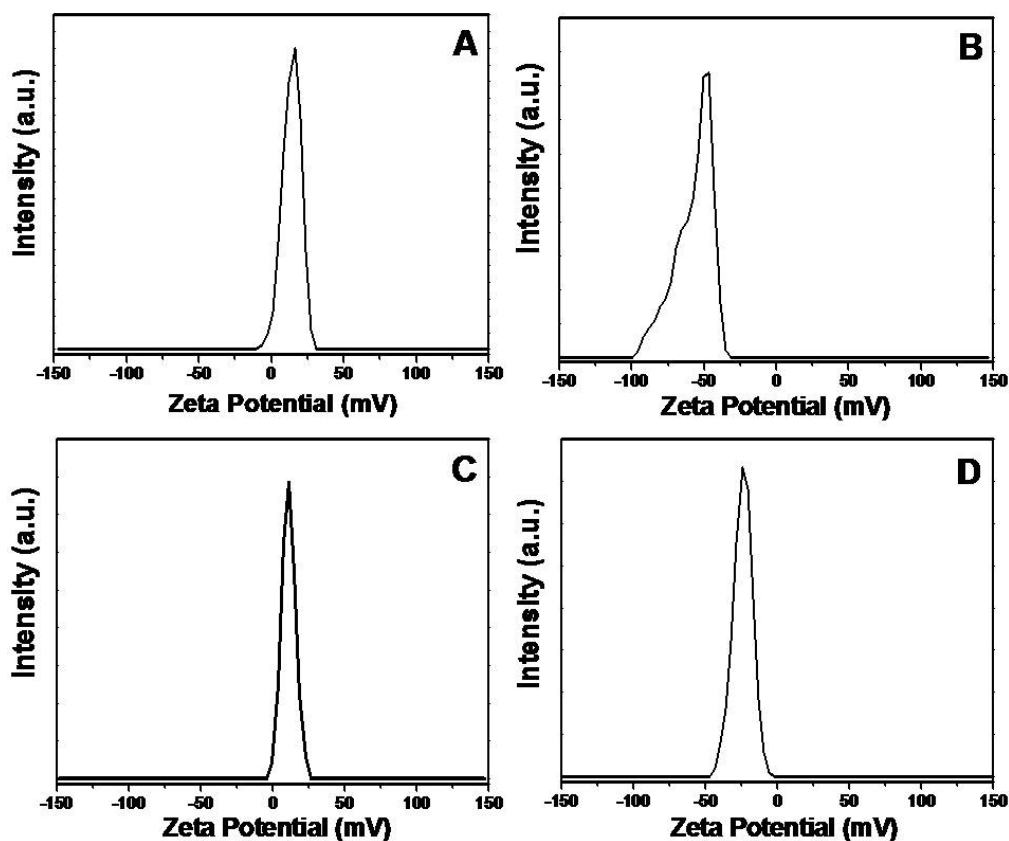


Fig. S6 The zeta potentials (ζ) of APTES modified Ag NWs (A), GO colloid (B), CdS NWs (C) and Ag NWs-GO (D) in deionized water without adjusting pH values.

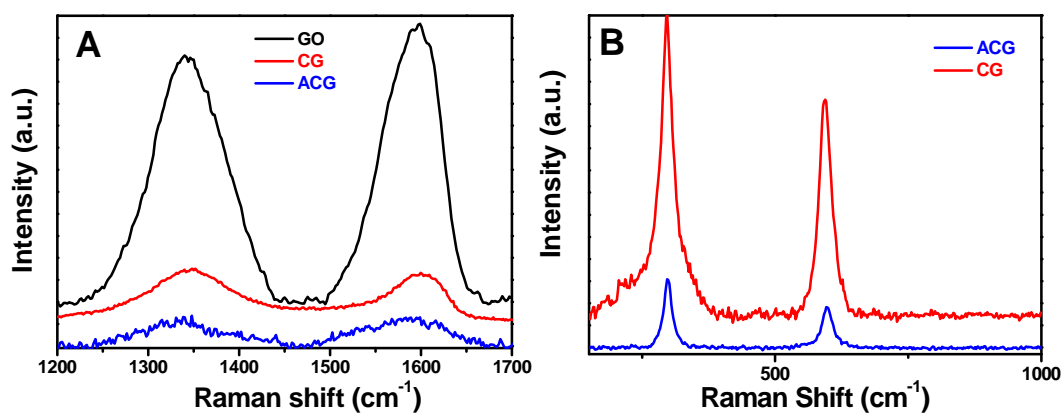


Fig. S7 Raman spectra of GO, CG, and ACG, showing the presence of G and D bands (A) and raman spectra of CG and ACG, showing the presence of Cd-S bond (B).

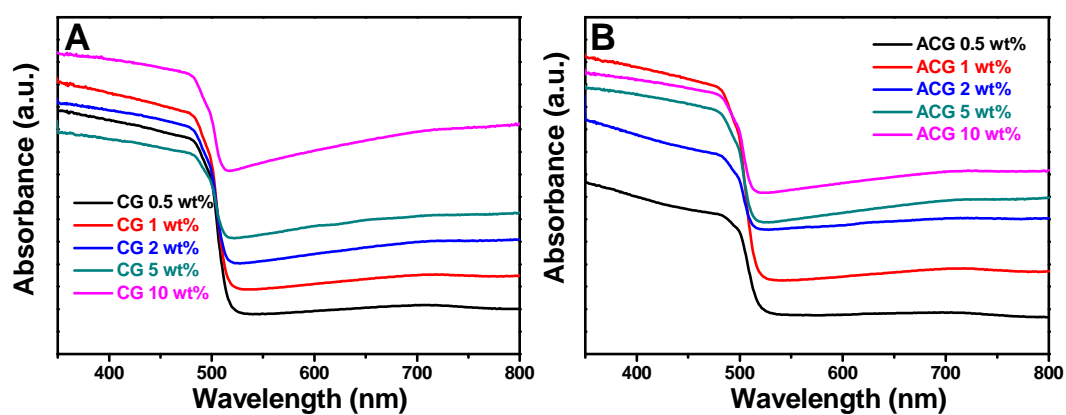


Fig. S8 UV-vis diffuse reflectance spectra (DRS) of CG (A) and ACG (B) with different weight addition ratios of RGO and Ag NWs-RGO.

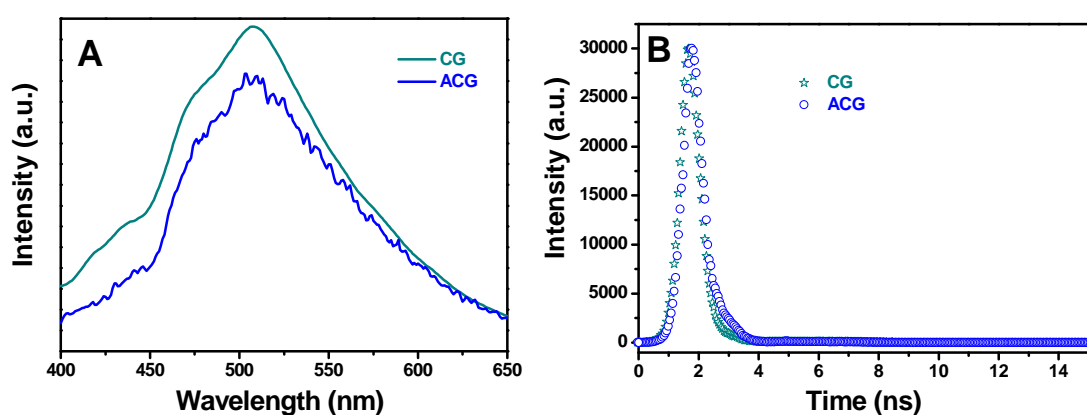


Fig. S9 Photoluminescence (PL) spectra and PL decay of the samples.

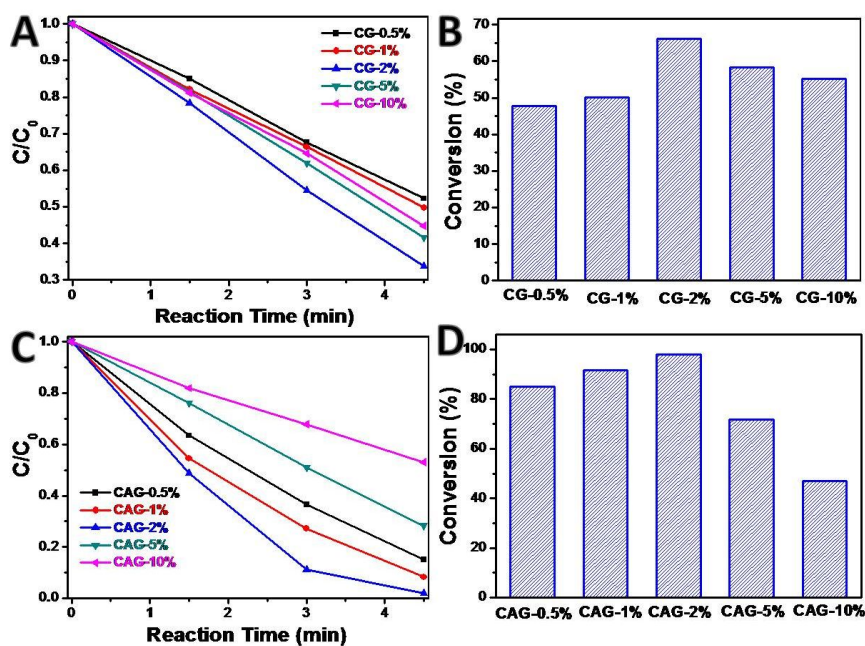


Fig. S10 Photocatalytic performances of CG (A and B), and ACG (C and D) with different weight addition ratios of RGO and Ag NWs-RGO for reduction of 4-nitroaniline under visible light ($\lambda > 420$ nm) irradiation.

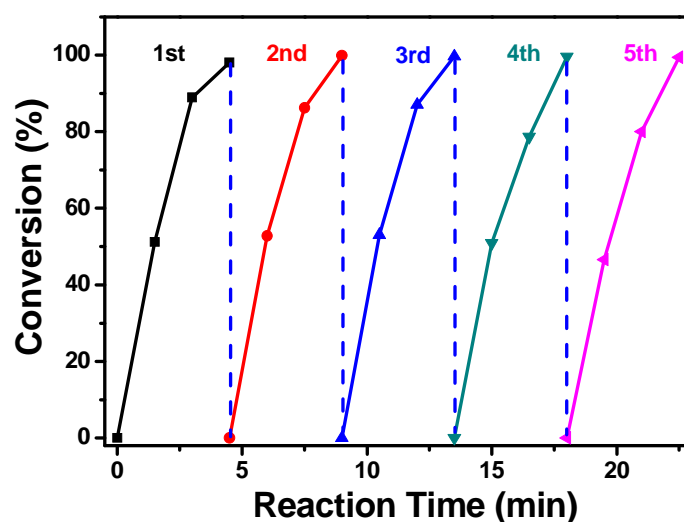


Fig. S11 Recycling photocatalytic reduction of 4-nitroaniline over ACG under visible light irradiation ($\lambda > 420$ nm).

References

- S1. S. Liu, M.-Q. Yang and Y.-J. Xu, *J. Mater. Chem. A*, 2014, **2**, 430.
- S2. L. Wang, H. Wei, Y. Fan, X. Gu and J. Zhan, *J. Phys. Chem. C*, 2009, **113**, 14119.
- S3. S. Liu, Z. Chen, N. Zhang, Z.-R. Tang and Y.-J. Xu, *J. Phys. Chem. C*, 2013, **117**, 8251.
- S4. S. Liu and Y.-J. Xu, *Nanoscale*, 2013, **5**, 9330.
- S5. D. C. Marcano, D. V. Kosynkin, J. M. Berlin, A. Sinitskii, Z. Sun, A. Slesarev, L. B. Alemany, W. Lu and J. M. Tour, *ACS Nano*, 2010, **4**, 4806.
- S6. J. Jiu, T. Araki, J. Wang, M. Nogi, T. Sugahara, S. Nagao, H. Koga, K. Suganuma, E. Nakazawa, M. Hara, H. Uchida and K. Shinozaki, *J. Mater. Chem. A*, 2014, **2**, 6326.